Received: 15 May 2017 | Revised: 16 August 2017 | Accepted: 7 September 2017

DOI: 10.1002/qua.25497

FULL PAPER

WILEY International Journal of QUANTUM CHEMISTRY

DFT study of the acid-catalyzed esterification reaction mechanism of methanol with carboxylic acid and its halide derivatives

Monsurat M. Lawal[1] | Thavendran Govender[1] | Glenn E. M. Maguire[1,2] | Hendrik G. Kruger[1] | Bahareh Honarparvar[1]

[1]Catalysis and Peptide Research Unit, School of Health Sciences, University of KwaZulu-Natal, Durban 4041, South Africa

[2]School of Chemistry and Physics, University of KwaZulu-Natal, Durban 4041, South Africa

Correspondence
Bahareh Honarparvar, Catalysis and Peptide Research Unit, School of Health Sciences, University of KwaZulu-Natal, Durban 4041, South Africa.
Email: Honarparvar@ukzn.ac.za

Funding information
College of Health Sciences, University of KwaZulu-Natal, Asphen Pharmacare, Medical Research Council, and National Research Foundation (South Africa)

Abstract

Extensive experimental studies have been dedicated to the esterification mechanisms from carboxylic acids and acid halides. However, attention on the theoretical aspect of the mechanism has been scarcely addressed. Herein, the acid-catalyzed esterification mechanism of methanol with acetic acid and its halide derivatives is described using density functional theoretical method and solvation model based on density. The mechanistic investigation involved formation of cyclic pre-reaction and 6-membered ring transition structures, which favors the esterification process and product formation. A good comparison with experimental data from literature for the esterification reaction of acetic acid with methanol was achieved through this in silico approach. Density Functional Theory-based quantum descriptors were applied to provide a better understanding on the reactivity, selectivity, and stability of this reaction. This theoretical results provide a crucial guide to study classical acid-catalyzed reaction mechanisms and applying a reasonable theoretical model to study similar organic reactions. In addition, it can be applied to larger systems such as enzymatic mechanism.

KEYWORDS
acetic acid (HOAc), acetyl halides (XAc), Density Functional Theory (DFT), esterification reaction

1 | INTRODUCTION

Esters remained important intermediates in the chemical industry due to their widespread pharmaceutical applications and biodiesel production. Dating back to the 1890s, the Fischer esterification[1] reaction has remained a crucial process through which esters are formed via dehydrative coupling of carboxylic acids (RCOOH) with alcohol (ROH) in the presence of inorganic liquid acids.[2–4] Among studies on kinetics and mechanism of acid-catalyzed RCOOH esterification, methyl acetate (MeOAc) formation from acetic acid (HOAc) and methanol (MeOH) using homogeneous and heterogeneous acid catalysts are abundant.[4–6]

Rönnback et al.[2] had earlier hypothesized the nature of the acid-catalyzed esterification of HOAc with MeOH as a stepwise model involving 7 transition structures and 3 intermediates in acidic solution. This experimental study[2] was novel and serves as a basis for subsequent investigations. The overall reaction process is presented as:

$$CH_3COOH + CH_3OH \overset{H_3O^+}{\Longleftrightarrow} CH_3COOCH_3 + H_2O \quad (1)$$

The production of MeOAc from HOAc and MeOH has been kinetically mediated by homogeneous[2,6–11] or heterogeneous catalysts,[5,6,12–15] with more research being performed on the latter due to increased reusability,[16] high selectivity,[17] and less product contamination.[6,16,18] The synthesis and kinetics via microwave, membrane, batch, and microchannel reactors have also been addressed.[12,13,19,20] Most recent experimental investigations (from 2011) have reported free energy of activation for this process with values ranging from ~7.7 to 15.1 kcal mol^{-1}[4–6,15,21–26] in

different reaction media/solvents at temperature up to 333 K. In addition to this parameter, some studies also provided heat of reaction (enthalpy, ΔH) and entropy (ΔS) of activation values within −1.0 and 0.1 kcal mol^{-1}[6,21,25] for ΔH while 1.0 E^{-5} and 0.1 cal $(mol\ K)^{-1}$ for the reaction entropy.[22,25]

A theoretical free energy barrier of 22.4 kcal mol^{-1} in solution for this same reaction was reported and described in a stepwise model involving 4 TS structures and 3 intermediates by Pliego and coworkers[27] using

$$CH_3COOH^+CH_3OH_2^+(CH_3OH)_2 \leftrightarrow\ CH_3C(OH)OCH_3^+(CH_3OH)_2 +\ H_2O. \tag{2}$$

Alcoholysis of acid anhydrides [$(RCO)_2O$] and acyl chlorides (RCOCl) are also used to obtain esters, with the latter more commonly studied.[28] Applications of $(RCO)_2O$ and RCOCl in regioselective protection of compounds with multifunctional groups are also well established.[29–33]

Lately, we have proposed three possible models for the uncatalyzed esterification reaction of acetic acid and acetyl halides using a M06-2X/def2-TZVP theoretical model.[34] The Density Functional Theory (DFT) method and basis set were selected after careful examination of three density functionals and seven basis sets (Supporting Information). The mechanism involves one-step 4-membered ring, and 4 different conformations of 6-membered ring transition state (TS) structures; including one-step and two-step concerted mechanism (Figure 1). From the proposed TS models, it was observed that the one-step 6-membered (TS-6.1.1-X) concerted pathway exhibited the lowest energy barrier for acetyl chloride, bromide, and iodide. The outcome[34] is consistent with an earlier theoretical observation of no discernible formation of a tetrahedral intermediate in the S_N2 reaction of acetyl chloride with 6 methanol molecules.[31] The results support earlier assumptions that the alcoholysis of acetyl chloride hardly proceed as a stepwise mechanism. Meanwhile, a two-step concerted model involving formation of 2 cyclic precomplexes, a tetrahedral intermediate, and 2 six-membered ring TS structures was preferred for HOAc and its fluoride analogue. The estimated theoretical free activation energies corroborates with experimental values.[34]

In addition, an autocatalysis process was examined[34] for the reaction of HOAc with MeOH ($2CH_3COOH + CH_3OH$). A solution phase free energy of activation of approximately 33 kcal mol^{-1} was obtained for a similar (uncatalyzed) cyclic transition state structure (TS-6.2.4-OH) (Figure S1 and data provided in the Supporting Information). In all cases, the concerted processes involve formation of prereaction complexes[34] that facilitate the structural formation of the cyclic TSs.

Cyclic TS structures have been found to be energetically plausible as reported by our group during the acetylation of anhydride with methanol.[29,30] The 6-membered ring TS structures reported were related to a system first reported by Yamabe and Ishikawa on investigating the hydrolysis of acetic anhydride.[35] These TS structures seem similar to pseudo-pericyclic transition structures reported previously by Birney and coworkers.[36–38]

Herein, a single cyclic reaction mechanism for all the acids (acetic acid and acetyl halides) based on Equation 1 is reported with the DFT method and def2-TZVP basis set. This was proposed to occur in a concerted mechanism involving 2 molecules of MeOH and 1 protonated XAc passing through one-step 6-membered cyclic (as in TS-6.1.1-X in Figure 1). Illustrated in Figure 2 is the proposed reaction profile for this mechanism for all the selected acids, XAc (where X = OH, F, Cl, Br, and I). The theoretical solution phase free activation energy obtained for the acid-catalyzed esterification reaction of acetic acid plus methanol is in agreement with experimental values. Commonly used quantum chemical quantities are also applied to provide an in-depth understanding of this intermolecular reaction mechanism.

2 | COMPUTATIONAL DETAILS

2.1 | Thermochemistry and kinetics

To achieve more realistic results with computational modeling of reactions, solvent effects are of great importance. Solute–solvent interactions are required to modify the structure, energy, and total behavior of systems. A number of methods have been established[27,39–41] to estimate thermochemistry parameters in solution. Rate constant k, which is the measure of the change in concentration of the reactants or products per unit time, was obtained from Equation 5 and taking the natural logarithm, we report as ln *k*. Variables k_B, *h*, and *R*, are Boltzmann, Planck, and gas constants, respectively, while *T* is the temperature in Kelvin and *c* is the concentration. ΔG_{sol}, ΔG_g, and $\Delta\Delta G_{solv}$ are the calculated solution phase free energy, gas phase free energy, and bulk solvent contribution, respectively, at 1 M standard state for all species (Equation 3) while ΔG^0_{sol} is the observable solution phase free activation energy at 1 M (1 mol L^{-1}) concentration of solute and pure solvent (MeOH) as stated in Equation 4.[40] The entropy penalty ($nRT\ \ln[MeOH] = 1.9$ kcal mol^{-1}) was been paid for through the subtraction of its correction to compress the concentration in solution to 1 M.[40]

$$\Delta G_{sol} = \Delta G_g + \Delta\Delta G_{solv,} \tag{3}$$

$$\Delta G^0_{sol} = \Delta G_{sol} - nRT\ \ln[MeOH], \tag{4}$$

$$k = \frac{k_B T}{hc^0}\ \exp\left(-\frac{\Delta G^{\ddagger}}{RT}\right). \tag{5}$$

All calculations were performed using Gaussian 09 program.[42] To confirm that the results obtained are not an artifact of a specific level of theory or basis set, 5 different hybrid density functionals, namely, B3LYP,[43,44] X3LYP,[45], B3PW91,[43,46] M06-2X, and M06-L,[47,48] and seven

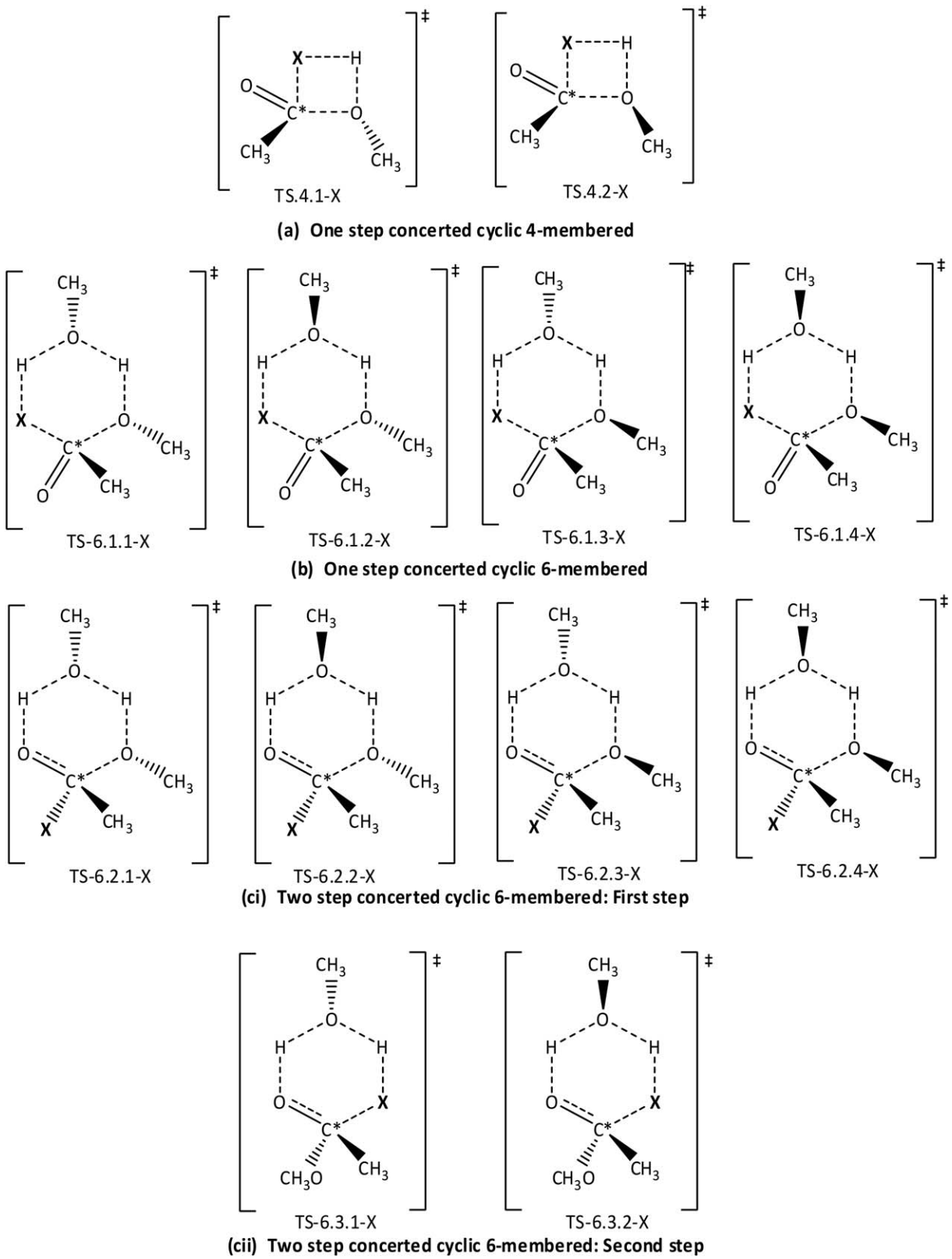

FIGURE 1 Previously studied cyclic transition state structures[34]

basis sets: 6–31 + G(d),[46,49,50] def2-TZVP,[51,52], aug-cc-pVTZ,[53,54] LANL2DZ,[55–57] def2-TZVP,[51,52] MidiX,[58,59] and DGDZVP[60,61] were examined (Supporting Information). The dispersed functional, M06-2X,[47,48] was observed to be sufficient and accurate in predicting the activation parameters for acetic acid (results are available in the Supporting Information). Also, this functional has been noted to be accurate in calculating the

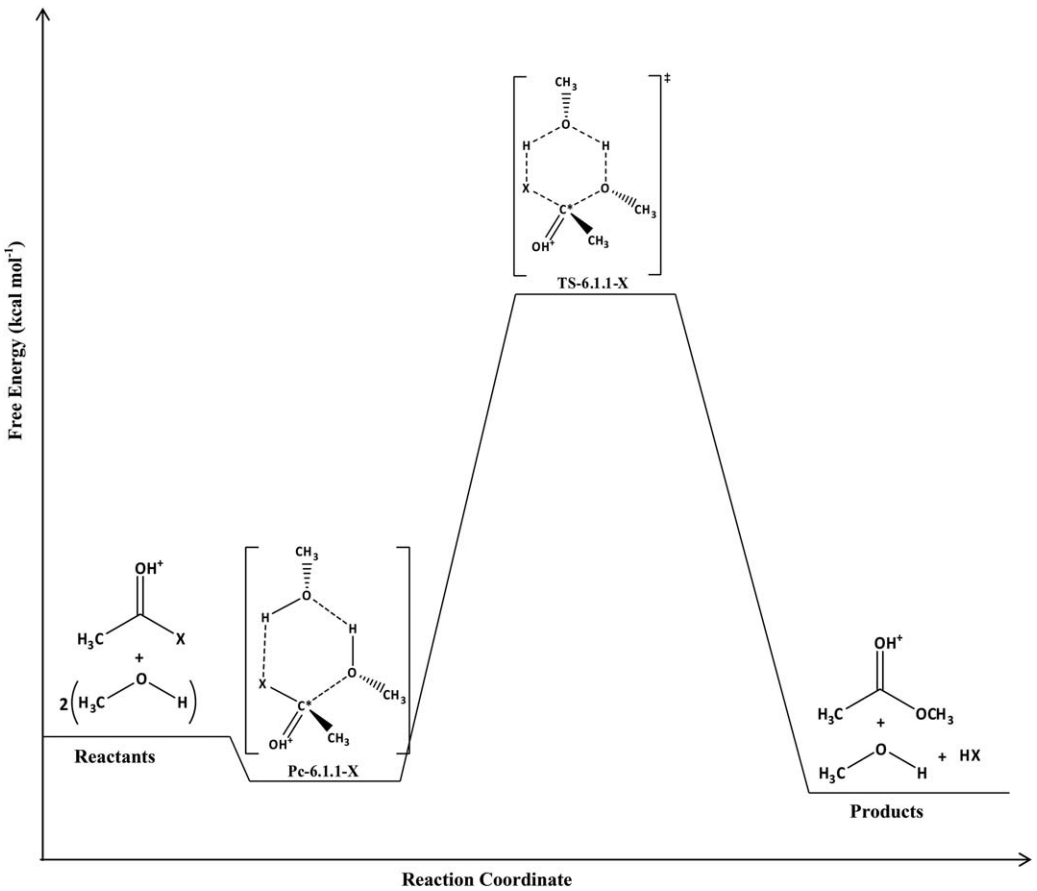

FIGURE 2 Possible mechanistic pathways including cyclic reacting species for the acid-catalyzed esterification of acetic acid and acetyl halides with 2 methanol molecules

thermochemistry of systems containing carbon, oxygen and halogen atoms.[34,48] One of the def2 series basis functions, def2-TZVP[51,52] was observed to give optimum results for the uncatalyzed esterification mechanism,[34] this was coupled with the selected M06-2X DFT model. Therefore, the combination of M06-2X/def2-TZVP model was used for the remainder of this study.

Calculations proceeded with full geometry optimization of reactants, precomplexes, products and TS structures along with frequency calculations for each reaction in gas and in solvent (MeOH) using solvation model based on density (SMD).[41]

Vibrational frequencies[62] at the same level and basis set were computed for the various unconstrained species to characterize them as local minima and TS structures (one-negative eigenvalue) on the potential energy surface (PES). Intrinsic reaction coordinates (IRCs)[63] were computed to verify the transition structures are truly the lowest saddle points connecting the expected structures on the reaction pathway. GaussView 5.0.8[64] was used as preprocessor and postprocessor visual interface for this study.

2.2 | Quantum properties

The conceptual quantum chemical descriptors were derived from energies of the frontier molecular orbitals (FMOs);[65] highest occupied molecular orbital (E_{HOMO}), and lowest unoccupied molecular orbital (E_{LUMO}), respectively. The studied quantities for the TS structures in implicit water were ionization potential (IP),[66] electron affinity (EA),[66] band gap (ΔE), chemical hardness (η),[67] global softness (S),[67] electronegativity (χ),[68] electrochemical potential (μ),[68] and electrophilicity index (ω)[69] (Equations 6–13).

Another computational parameter for predicting chemical reactivity is molecular electrostatic potential (MESP).[70] Examining the ESP of the reacting species along the PES of acid-catalyzed esterification of methanols with acetic acid and its halide analogues provides a deep insight on the reactivity of these molecules.[71] The MESP of the reactants, TS complexes and products were computed using SMD/M06-2X/def2-TZVP and by specifying the Breneman CHelpG Electrostatic Potential-Derived Charges keyword.[72]

$$\text{Ionization potential (IP)} = -E_{HOMO}, \tag{6}$$

$$\text{Electron affinity (EA)} = -E_{LUMO}, \tag{7}$$

$$\text{Band gap } (E) = E_{\text{HOMO}} - E_{\text{LUMO}}, \tag{8}$$

$$\text{Chemical hardness } (\eta) = \frac{E_{\text{LUMO}} - E_{\text{HOMO}}}{2}, \tag{9}$$

$$\text{Global softness } (S) = \frac{1}{\eta}, \tag{10}$$

$$\text{Chemical potential } (\mu) = -\frac{\text{IP} + \text{EA}}{2}, \tag{11}$$

$$\text{Electronegativity } (\chi) = -\mu, \tag{12}$$

$$\text{Electrophilicity index } (\omega) = \frac{\mu^2}{2\eta}. \tag{13}$$

3 | RESULTS AND DISCUSSION

3.1 | Reaction mechanism and activation parameters for the acid-catalyzed esterification reaction of methanol with acetic acid and acetyl halides

The thermodynamics and kinetics for the reactions of acetic acid and its halide analogues with methanol to form ester (methyl acetate) are presented in Table 1. All values are reported relative to the sum of separated reactants. Reporting the energetics of the TS structures relative to the sum of separated reactants and not with respect to prereaction complexes was based on the fact that in the typical experiment procedure,[7] the precomplex or its relative energy are not considered per se.

Generally, the esterification of acetic acid and acetyl halides with two molecules of methanol in the presence of acid (H^+) followed the proposed concerted models (Figure 2). This involves the orientation of the reactants in an ordered model leading to the formation of a cyclic prereaction complex, which facilitates the 6-membered ring TS structure hence, favoring the formation of products in a 1 TS process (Figure 2). The reaction pathway follows the same pattern akin to the one-step concerted 6-membered cyclic uncatalyzed esterification mechanism (Figure 1b).

Briefly, the acid-catalyzed esterification reaction involves a concerted mechanism in which 2 hydrogen atoms are transferred within the cyclic ring and a reduced methanol (CH_3O^-) makes a π attack on the C═O bond of the acids. It is fascinating to note that this attack led to the conversion of C═O to C—O in HOAc and FAc while reluctance was observed in ClAc, BrAc, and IAc with respect to this occurrence (Figure 3). The behavior of these acids with larger halides corresponds to earlier experimental[73,74] and theoretical[31] observations that the methanolysis of acetyl chloride does not obey the popularly assumed addition-elimination pathway. Even in the presence of solvent, the C═O of ClAc, BrAc, and IAc resists conversion to a C—O single bond (Figure 3). Consequently, the C–X (X = Cl, Br, and I) bond strength and the stability of the leaving group have a profound effect upon the mechanism of esterification reactions in these acids.[31]

Presented in Table 1 are the activation parameters for the acid-catalyzed esterification reactions of the selected acids. The Gibbs free energy profile of the overall process in solution is presented in Figure 4. Estimation of the total heat content of any system gives rise to enthalpy (*H*) while the degree of disorderliness in a reaction is denoted by entropy (*S*).[75] The Gibbs free energy (*G*) of a compound is temperature dependent; it incorporates both enthalpy and entropy of a system. The *G* of a reacting entity can be obtained through the difference between *H* and *S* at a given temperature. Other quantities are defined in the methodology section (see section 2).

In vacuum, the estimated theoretical enthalpies (ΔH^a) of the precomplexes range from −17.0 to −47.5 kcal mol^{-1} (Table 1) while solvating these systems implicitly in methanol using SMD method lowered the enthalpy (ΔH^b) penalties greatly with value up to 17 kcal mol^{-1} (Pc-6.1.1-F; Table 1). In both media, Pc-6.1.1-OH has the most positive enthalpy values, which denotes its less spontaneity with respect to bond formation compared to the halides. The calculated entropy values of the prereaction complexes contrast observations in the enthalpy data. Entropy penalties increased (except Pc-6.1.1-I) in methanol compared to gas phase with values ranging from −64 to −80.6 cal $(mol\ K)^{-1}$ (ΔS^b, Table 1).

For the studied esterification reactions, the free energies in gas phase (ΔG^a) for the precomplexes were highly exergonic while bulk solvent (methanol) contributed free energies ranging from −3.2 to 16 kcal mol^{-1} ($\Delta\Delta G^c_{solv}$; Table 1). At 1 M standard concentrations for all the species in solvent, the free energies (ΔG^d_{sol}) were exergonic for the acid halides while HOAc remained positive with 10.4 kcal mol^{-1}, which arises from its slightly positive Gibbs free energy in vacuum. When the effects of entropy, temperature, and reaction rates were incorporated, the observable Gibbs free energy at 1 mol L^{-1} for solute and pure solvent for methanol ($\Delta G^{0\ e}_{sol}$) of these precomplexes became more exergonic (Table 1 and Figure 4). However, the HOAc reaction has a positive precomplex value (9.84 kcal mol^{-1}) for $\Delta G^{0\ e}_{sol}$, an observation similar to the uncatalyzed system.[34] This may be rationalized as a result of the reduced chemical reactivity of the acetic acid in relation to the acid halides.

A careful observation of the reaction enthalpies and entropies of the TS structures showed a decrease in penalties and increase in stability on moving from vacuum to solvent phase (TS-6.1.1-X, X = OH, F, Cl, Br, and I; Table 1). The theoretical heat of reaction in solvent (ΔH^b) for the acid-catalyzed esterification of HOAc and MeOH was −8.5 kcal mol^{-1} (Table 1) while reported experimental values are within −1.0 to 0.1 kcal mol^{-1},[6,21,25] for this same reaction. Activation free energy barriers in gas phase (ΔG^a) were exergonic with HOAc and BrAc having the highest (–3.9 kcal mol^{-1}) and the lowest (–24.8 kcal mol^{-1}) values, respectively (TS-6.1.1-X [X = OH and Br]; Table 1).

TABLE 1 Relative thermodynamic and kinetic parameters (Figure 2) for the one-step cyclic esterification of acids with methanol using $CH_3C(OH)^+X$ (X = OH, F, Cl, Br, and I) + $2CH_3OH$ as reference reactants at M06-2X/def2-TZVP theoretical model and 298.15 K

	ΔH^a	ΔS^a	ΔG^a	ΔH^b	ΔS^b	$\Delta\Delta G_{solv}{}^c$	$\Delta G_{sol}{}^d$	$\Delta G^0_{sol}{}^e$	ln *k*
Reactants	0.00	0.00	0.00	0.00	0.00	0.00	0.00	0.00	...
Pc-6.1.1-OH	−17.00	−61.54	1.35	−6.13	−72.20	10.40	11.74	9.84	...
TS-6.1.1-OH	−29.48	−85.78	−3.91	−8.46	−84.47	21.77	17.87	15.97	2.50
Products	−7.67	−1.81	−7.13	−3.65	−8.15	4.51	−2.62	−4.52	...
Reactants	0.00	0.00	0.00	0.00	0.00	0.00	0.00	0.00	...
Pc-6.1.1-F	−47.48	−73.71	−25.50	−30.31	−80.55	16.01	−9.49	−11.39	...
TS-6.1.1-F	−38.80	−82.15	−14.31	−29.36	−81.66	21.33	7.02	5.12	20.82
Products	−28.55	−4.09	−27.33	−23.10	−9.66	5.83	−21.60	−23.50	...
Reactants	0.00	0.00	0.00	0.00	0.00	0.00	0.00	0.00	...
Pc-6.1.1-Cl	−43.07	−73.52	−18.07	−30.12	−77.50	8.85	−9.21	−11.11	...
TS-6.1.1-Cl	−38.50	−81.02	−14.34	−27.46	−77.29	9.67	−4.67	−6.57	40.55
Products	−30.28	−0.08	−30.25	−27.91	−6.79	2.63	−27.72	−29.62	...
Reactants	0.00	0.00	0.00	0.00	0.00	0.00	0.00	0.00	...
Pc-6.1.1-Br	−37.57	−75.58	−12.88	−31.79	−78.96	−3.16	−9.72	−11.62	...
TS-6.1.1-Br	−47.69	−76.63	−24.85	−29.77	−80.25	15.59	−9.27	−11.17	48.31
Products	−32.78	0.08	−32.81	−29.12	−6.73	3.41	−29.40	−31.30	...
Reactants	0.00	0.00	0.00	0.00	0.00	0.00	0.00	0.00	...
Pc-6.1.1-I	−23.00	−66.74	−21.11	−8.99	−64.26	13.79	−7.31	−9.21	...
TS-6.1.1-I	−41.95	−79.13	−18.36	−26.04	−78.86	15.52	−2.84	−4.74	37.46
Products	−30.25	−0.12	−30.21	−23.19	−7.09	7.17	−23.14	−25.04	...

Values are reported in 2 decimal places relative to the sum of separated reactants. H and G are in kcal mol^{-1} while *S* is reported in cal $(mol\ K)^{-1}$.
[a]Standard state 1 mol L^{-1} for all species in gas phase.
[b]Thermochemistry from SMD/M06-2X/def2-TZVP model.
[c]Bulk solvation free energy with SMD/M06-2X/def2-TZVP.
[d]Standard state at 1 mol L^{-1} for all species in methanol.
[e]Standard state at 1 mol L^{-1} for solute and pure solvent for methanol.

Solvating these moieties in methanol implicitly gave free energy ($\Delta\Delta G^c_{solv}$) values ranging from 9.7 to 22 kcal mol^{-1} while the calculated and observable solution phase free energies (ΔG^d_{sol} and $\Delta G^0_{sol}{}^e$) are within −11 and 18 kcal mol^{-1} (Table 1). The ln *k* values ranges from 2 to 48. At 1 M standard states for solute and pure solvent, the free energy barrier and the rate constant value of approximately 16 kcal mol^{-1} and 2.5, respectively, were deduced for acid-catalyzed esterification of acetic acid with methanol. These data are in agreement with a recent experiment study in which homogeneous acid catalyst was used and an activation free energy of 15.1 kcal mol^{-1} was reported.[6] Using Equation 5, the calculated ln *k* is 4.0.

A related theoretical study was reported by Silva et al.[27] with a theoretical $\Delta G^0_{sol}{}^e$ of activation value of 22.4 kcal mol^{-1} in a stepwise mechanism, using hybrid cluster continuum model. They used the following overall mechanism to calculate the relative energy differences:

$$CH_3COOH^+CH_3OH_2^+(CH_3OH)_2 \leftrightarrow\ CH_3C(OH)OCH_3^+(CH_3OH)_2 +\ H_2O. \tag{14}$$

While reproducing their[27] rate-limiting TS (TSb-3) using the same approach as reported by these authors (column B and C; Table 2 and Figure 5), we obtained similar energies and bond distances; the small discrepancies can be attributed to the choice of calculation parameters. Column A are energies of TSb-3 from Silva et al. work[27] at X3LYP/6−31 + G(d) level while B presents our reproduced TSb-3 with the same level of theory [X3LYP/6−31 + G(d)] and reference substrates. When we applied M06-2X/def2-TZVP level of theory to TSb-3, values in column C were obtained. Column D represents the values obtained from the cyclic TS-6.1.1-OH with M06-2X/def2-TZVP model when the reaction is

$$CH_3C(OH)OH^+ + 2\ CH_3OH \underset{\Delta}{\Longleftrightarrow} CH_3C(OH)OCH_3{}^+ + CH_3OH + H_2O. \tag{15}$$

When the cyclic rate determining step (TSb-3) by Pliego and coworkers was compared with the possible diastereomeric options studied for the uncatalyzed model, it was found to match the geometry of TS-6.1.3-OH (Figure 1) which is less feasible (than TS-6.1.1-OH) due to steric hindrance.

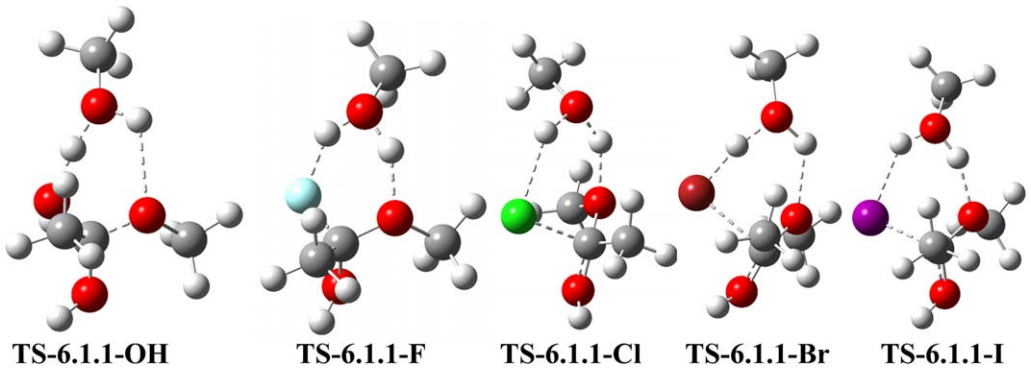

FIGURE 3 Optimized transition state structures for the acid-catalyzed esterification reaction of acetic acid and its halide derivatives using SMD/M06-2X/def2-TZVP theoretical model

The IRCs for both TS3-b (Table 2, columns A–C) and TS-6.1.1-OH (Table 2, column D) gave the same reactants and products. Bond length distance of 1.39 Å (Figure 5, M06-2X/def2-TZVP) between the carbonyl carbon and methanol for TS-6.1.1-OH is in good agreement with a distance of 1.42 Å [X3LYP/6–31 + G(d)] reported by these authors.[27]

It is quite interesting to note that the corresponding theoretical $\Delta G^{0}_{sol}{}^{d}$ for the uncatalyzed mechanism at M06-2X/def2-TZVP theoretical level (TS-6.1.1-OH, Figure 1) was 40.5 kcal mol^{-1}.[34] In other words, acid catalysis accounts for a very large decrease in the activation energy (up to 22 kcal mol^{-1}) in solution. For the corresponding uncatalyzed TS of acetyl fluoride (TS-6.1.1-F),[34] a solution phase free energy of 32.05 kcal mol^{-1} was estimated, thus acid catalysis accounts for a 27 kcal mol^{-1} reduction in the energy barrier ($\Delta G^{0}_{sol}{}^{d}$ of TS-6.1.1-F, Table 1). This observation buttressed an earlier experimental report by Bunto and Fendler[76] on increased reactivity of FAc when hydrolyzed in the presence of a catalytic amount of acid (H^{+}).

Although the reaction of ClAc, BrAc, and IAc usually proceeds without acid catalyst mediation, it is clear from experimental conditions[2] and the general reaction mechanism that acid is generated during the reaction. Protonation of the carbonyl oxygen of this acid leads to a reduction of the activation barrier to values between −4.7 and −11.1 kcal mol^{-1} (Table 1) compared to values ranging from 19 to 22 kcal mol^{-1} for the uncatalyzed model.[34] The negative solution phase free energy obtained buttressed the nonrequirement of acid catalyst in the esterification reaction of these acid halides. The overall pathway leading to product remains exergonic in all cases.

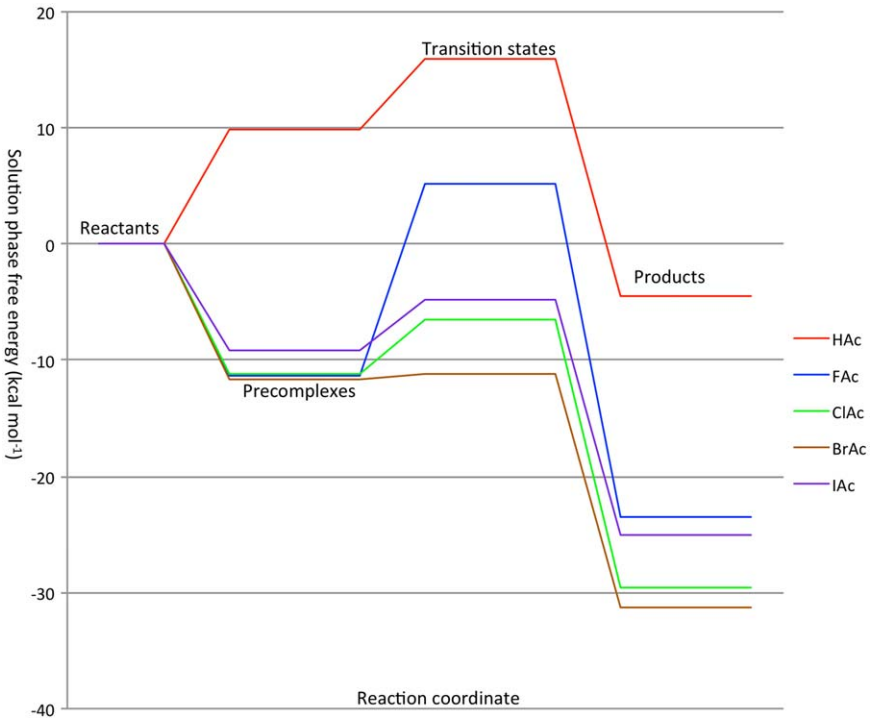

FIGURE 4 Gibbs free energy profile (in solution) of the acid-catalyzed esterification of acetic acid and acetyl halides with methanol at M06-2X/def2-TZVP level of theory. Various TS structures are presented in Figure 3

TABLE 2 Thermodynamic properties for the reaction and activation of acid-catalyzed esterification of acetic acid in methanol (Equations 5 and 6)

	A	B	C	D
ΔG_{CPCM}	24.84	22.61	20.82	12.77
ΔG^{a}	20.40	20.17	23.44	−3.91
$\Delta\Delta G_{solv}{}^{b}$	0.11	0.71	1.20	21.77
$\Delta G_{sol}{}^{c}$	20.51	20.88	24.64	17.87
$\Delta G^{0}_{sol}{}^{d}$	22.40	22.78	26.54	15.97

All values are reported in kcal mol^{-1} at 298.15 K in 2 decimal places.
Columns A-D; A are energies of TSb-3 from Silva et al. work [27] at X3LYP/6–31+G(d) level. B is the reproduced TSb-3 with the same level of theory [X3LYP/6–31+G(d)] and referenced [27] substrates. C equals values with M06-2X/def2-TZVP level of theory for TSb-3. D represents the values obtained from the cyclic TS-6.1.1-OH with M06-2X/def2-TZVP studied model.
[a]Standard state 1 mol L^{-1} for all species in gas phase.
[b]Solvation free energy with SMD.
[c]Standard state at 1 mol L^{-1} for all species in methanol.
[d]Standard state at 1 mol L^{-1} for solute and pure solvent for methanol.

3.2 | DFT-based chemical reactivity descriptors for the acid-catalyzed esterification reaction of acetic acid and acetyl halides with methanol

The application of DFT-based quantum chemical properties to shine more light on the preference of chemical reactions at the molecular level remained substantial.[77] For many stable models, the gap between the energies of the highest occupied molecular orbital (HOMO) and lowest unoccupied molecular orbital (LUMO) defines the electronic properties of such systems.[65] The energies of HOMO and LUMO are often referred to as the energies of the FMOs and can be applied to TS molecules to provide a vital basis for estimating the chemical reactivity, selectivity and stability of the TS structures studied herein.[34,77] The energies of the FMOs were calculated to study some quantum chemical parameters (Equations 6–13) for the five TS structures. Shown in Table 3 are results (in three decimal places) of the HOMO, LUMO energies and other derived parameters in methanol using SMD/M06-2X/def2-TZVP method. The lobes of the studied FMOs are provided in Figure 6.

It is established that, molecules with high E_{HOMO} values can easily donate their electrons compared to molecules with lower E_{HOMO} values.[65] E_{HOMO} ranges from −0.313 to −0.392 eV (Table 3) in the order: TS-6.1.1-F > TS-6.1.1-OH > TS-6.1.1-Cl > TS-6.1.1-Br > TS-6.1.1-I, an indication of electron donating abilities of these acids.[78] The plausibility of the starting materials to undergo termolecular process forming 6-membered cyclic TS structures can be traced to good intermolecular interaction within the acids and 2 methanol molecules. In bulk methanol, the TS structures have small values for E_{LUMO} (–0.027 to 0.049 eV) in the same order as in E_{HOMO} (Table 3). Based on these observations, it can be assumed that the reactivity of these systems can be related to the energy level of the HOMO and the interatomic charge transfer within the starting materials.[79]

As illustrated in Figure 6, the HOMO electrons are largely localized within the nucleophilic methanol and the first three acids (HOAc, FAc, and ClAc). Analysis of the spatial distribution of the HOMO on each functional group of the studied acids (Figure 6) reflects that the esterification mechanism with methanol is indeed dependent on the reactivity of these acids.[65] The shape of the mapped surface area of the LUMOs for TS-6.1.1-F and TS-6.1.1-OH are quite similar as reflected in their more positive LUMO values (Table 3), which can also be correlated to their energetics (Table 1). It is interesting to note that the localization of HOMO and LUMO on TS-6.1.1-Cl, TS-6.1.1-Br, and TS-6.1.1-I are similar to the mapped scope observed in the uncatalyzed model.[34]

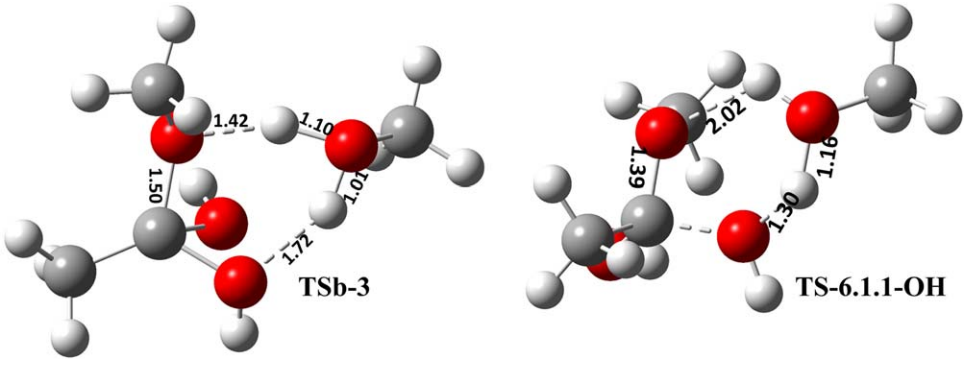

FIGURE 5 TSb-3 reproduced from literature[27] using X3LYP/6–31 + G(d) and our observed TS-6.1.1-OH model at M06-2X/def2-TZVP level of theory (Table 1)

TABLE 3 Conceptual quantum chemical descriptors for the transition state structures involved in the one-step concerted acid-catalyzed esterification reaction of acetic acid and acetyl halides with methanol using SMD/M06-2X/def2-TZVP

TSs	E_{LUMO} (eV)	E_{HOMO} (eV)	IP	EA	ΔE (eV)
TS-6.1.1-OH	0.044	−0.377	0.377	−0.044	0.422
TS-6.1.1-F	0.049	−0.392	0.393	−0.049	0.442
TS-6.1.1-Cl	0.008	−0.363	0.363	−0.008	0.371
TS-6.1.1-Br	−0.024	−0.329	0.329	0.024	0.306
TS-6.1.1-I	−0.027	−0.313	0.313	0.027	0.286
	μ (eV)	η (eV)	S (eV^{-1})	ω (eV)	χ
TS-6.1.1-OH	−0.166	0.211	4.742	0.066	0.166
TS-6.1.1-F	−0.171	0.221	4.526	0.066	0.171
TS-6.1.1-Cl	−0.177	0.185	5.389	0.084	0.177
TS-6.1.1-Br	−0.176	0.153	6.540	0.102	0.176
TS-6.1.1-I	−0.170	0.143	6.984	0.101	0.170

The nucleophilicity of a material can be determined by IP (Equation 6) while the electron withdrawing ability of a compound can be measured through EA.[66] IP follows the order; TS-6.1.1-F > TS-6.1.1-OH > TS-6.1.1-Cl > TS-6.1.1-Br > TS-6.1.1-I and EA gave an exactly opposite of the IP trend (Table 3). TS-6.1.1-F proved to have the highest potential to donate electrons. Band gap (ΔE) is usually obtained by taking the difference between E_{HOMO} and E_{LUMO} (Equation 8). It is an important stability index in molecular interaction description.[66] The smaller the band gap, the higher the probability of electron transfers within a given compound.[80] The increasing order of electron transfer in the TSs is TS-6.1.1-F < TS-6.1.1-OH < TS-6.1.1-Cl < TS-6.1.1-Br < TS-6.1.1-I, hence, TS-6.1.1-I is the most reactive acid. This observation is in agreement with accepted knowledge.

Within the context of the studied DFT-based quantum quantities, the global indices of reactivity displayed in Table 3 show that the electrochemical potential, hardness, softness, electrophilicity, and electronegativity data for the acid-catalyzed reaction of these acids with methanol leading to ester formation, follow reasonable trends. Electron movement is driven by the changes in electronegativity, while the hardness quantity is a measure of resistance of a system to chemical reactivity and selectivity, which results in flow of electrons from an occupied orbital to a previously unoccupied one.[66,67] The reluctance of these acids to react (based on the HOMO/LUMO results) resulted in the following order: TS-6.1.1-F < TS-

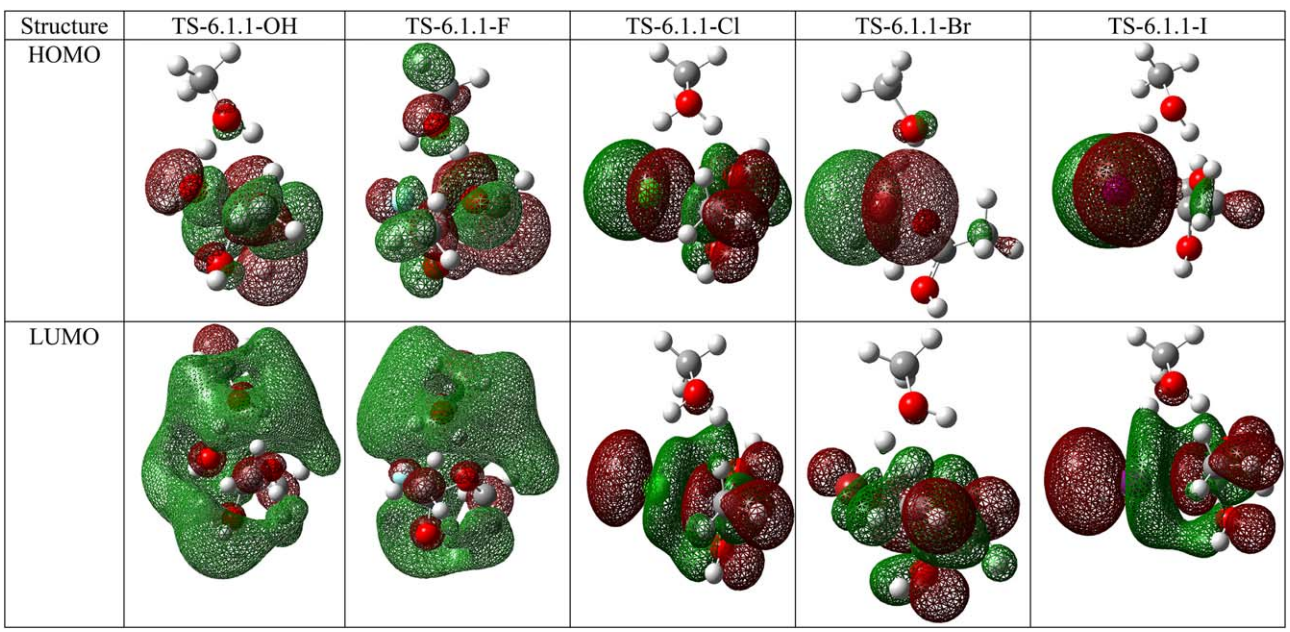

FIGURE 6 Frontier molecular orbitals (highest occupied molecular orbital [HOMO] and lowest unoccupied molecular orbital [LUMO]) of the TS structures involved in the one-step acid-catalyzed esterification reactions of acetic acid and acetyl halides with methanol at SMD/M06-2X/def2-TZVP level of theory

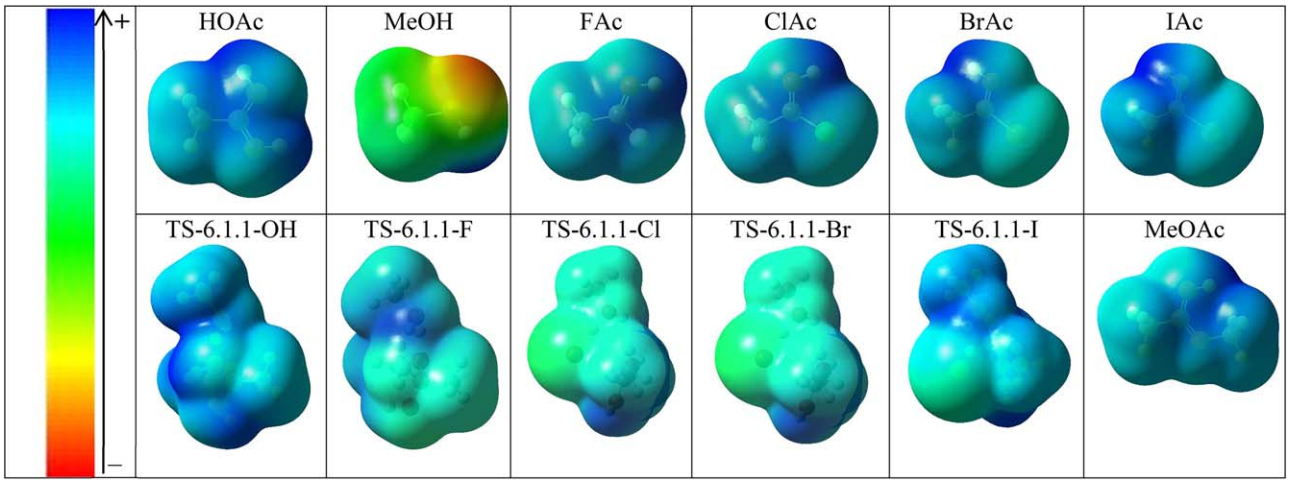

FIGURE 7 Electrostatic potential (ESP) surface of the TS structures involved in the one-step concerted acid-catalyzed esterification reaction of acetic acid and acetyl halides with methanol at SMD/M06-2X/def2-TZVP level of theory

6.1.1-OH < TS-6.1.1-Cl < TS-6.1.1-Br < TS-6.1.1-I; while chemical softness for these has an opposite trend (η and *S*, Table 3). Increase in the band gap value ultimately leads to a corresponding increase in the hardness and a decrease in the electrochemical potential (μ and η, Table 3). The electrophilicity of a system is measured by its global electrophilicity index (ω),[69] complexes with high electrophilicity index exhibit electrophilic characteristic. TS-6.1.1-Cl gave the highest (0.177) electronegativity value among other TS structures, while TS-6.1.1-OH showcased least electronegativity feature with value of 0.166 (Table 3).

Furthermore, the MESP surface of species along the reaction coordinates of the esterification reaction of acetic acid and acetyl halides were mapped to examine the intermolecular association of these acids with methanol. The electrostatic potential was mapped onto the self-consistent field (SCF)[81] of the total electron density. This method offers a unique way to visualize the behavior of molecules that tend towards positive and negative reactant species.[82] Presented in Figure 7 are the MESP charges for the separated reactants (protonated acids and methanol), product (protonated methylacetate) and the TS structures. The resulting overall ESP of the TS moieties leaves no doubt that these structures are attracted to the positively charged acids (Figure 7). It is quite interesting to observe that the estimated charge for all the TS complexes is within −0.232 and 0.232 e in which the reactivity order is TS-6.1.1-OH < TS-6.1.1-F < TS-6.1.1-I < TS-6.1.1-Cl < TS-6.1.1-Br and corresponding to the activation free energy (Figure 4 and Table 1).

4 | CONCLUSION

The esterification reactions of acetic acid and its halide analogues with methanol were studied in the presence of an acid catalyst using M06-2X hybrid density functional with def2-TZVP basis set. The reaction was modeled as a one-step concerted process involving 6-membered cyclic pre-complex and transition structures. The calculated solution phase free energy of activation for the esterification of acetic acid (of 15.9 kcal mol^{-1}) is in reasonable agreement with experiment (15.1 kcal mol^{-1}). The acid-catalyzed esterification of acid halides (X = Cl, Br, and I) with methanol suggests spontaneous reactivity (negative free energies of activation). For fluoride, the solution phase free energy (5 kcal mol^{-1}) also implies the spontaneous reactivity at room temperature. Molecules at room temperature have internal energy to overcome processes requiring between 15 and 20 kcal mol^{-1}.[83]

The studied DFT-based quantum properties proved to be helpful in studying the reactivity of the acids and stability of the TS structures. The advantage of this theoretical model is that it provides a single concerted mechanism for the acid-catalyzed esterification reactions between small organic acids/acid halides and methanol. It is likely that a linear reaction mechanism coexists with the cyclic one, where the respective proton transfers occur between the reactants and the protic solvent. However, more advanced software and theoretical model will be required that can accurately deal with solvent molecules at the ab initio/DFT level.

ACKNOWLEDGMENTS

The authors appreciate College of Health Sciences, University of KwaZulu-Natal, Asphen Pharmacare, Medical Research Council, and the National Research Foundation (South Africa) for financial support. We are also grateful to the Centre for High Performance Computing (www.chpc.ac.za) for computational resources.

ORCID

Bahareh Honarparvar http://orcid.org/0000-0001-9005-2282
Hendrik G. Kruger http://orcid.org/0000-0003-0606-2053

REFERENCES

[1] E. Fischer, A. Speier, *Chemistry* **1895**, *28*, 3252.
[2] R. Rönnback, et al., *Chem. Eng. Sci.* **1997**, *52*, 3369.
[3] J. Otera, J. Nishikido, *Esterification: Methods, Reactions, and Applications*, John Wiley & Sons, **2009**.
[4] Z. Zeng, et al., *Chem. Kinet.* **2012**, 255.
[5] E. Van de Steene, J. De Clercq, J. W. Thybaut, *J. Jpn. Assoc. Ion Exchange* **2014**, *25*, 234.
[6] M. Mekala, V. R. Goli, *Asia Pac. J. Chem. Eng.* **2014**, *9*, 791.
[7] H. A. Smith, *J. Am. Chem. Soc.* **1939**, *61*, 254.
[8] A. Kirby, *Compr. Chem. Kinet.* **1972**, *10*, 57.
[9] T. Pöpken, L. Götze, J. Gmehling, *Ind. Eng. Chem. Res.* **2000**, *39*, 2601.
[10] Y. Liu, E. Lotero, J. G. Goodwin Jr, *J. Catal.* **2006**, *242*, 278.
[11] M. B. Smith, J. March, *March's Advanced Organic Chemistry: Reactions, Mechanisms, and Structure*, 7th ed., John Wiley & Sons, Inc., Hoboken, NJ **2007**, Publication 2374.
[12] C. Zuo, et al., *Ind. Eng. Chem. Res.* **2014**, *53*, 10540.
[13] J. Vojtko, P. Tomčík, *Int. J. Chem. Kinet.* **2014**, *46*, 189.
[14] M. Mekala, V. R. Goli, *Chin. J. Chem. Eng.* **2015**, *23*, 100.
[15] S. Lux, et al., *Chem. Biochem. Eng. Q.* **2015**, *29*, 549.
[16] K. Suwannakarn, E. Lotero, J. Goodwin Jr, *Catal. Lett.* **2007**, *114*, 122.
[17] D. Y. Ganapati, H. M. Pranav, *Ind. Eng. Chem. Res.* **1994**, *33*, 2198.
[18] M. G. Kulkarni, A. K. Dalai, N. N. Bakhshi, *Bioresour. Technol.* **2007**, *98*, 2027.
[19] S. Assabumrungrat, et al., *Chem. Eng. J.* **2003**, *95*, 57.
[20] X. Yao, et al., *Catal. Lett.* **2009**, *132*, 147.
[21] Y.-T. Tsai, H.-m. Lin, M.-J. Lee, *Chem. Eng. J.* **2011**, *171*, 1367.
[22] P. E. JagadeeshBabu, K. Sandesh, M. B. Saidutta, *Ind. Eng. Chem. Res.* **2011**, *50*, 7155.
[23] S. Miao, B. H. Shanks, *J. Catal.* **2011**, *279*, 136.
[24] M. B. Mandake, S. V. Anekar, S. M. Walke, *Am. Int. J. Res. Sci. Technol. Eng. Math.* **2013**, *3*, 114.
[25] M. Mallaiah, G. V. Reddy, *Kinet. Catal.* **2015**, *56*, 419.
[26] M. Mekala, V. R. Goli, *Prog. React. Kinet. Mech.* **2015**, *40*, 367.
[27] P. L. Silva, et al., *Theor. Chem. Acc.* **2015**, *134*, 1591.
[28] T. Willms, et al., *Thermochim. Acta* **2000**, *364*, 35.
[29] H. G. Kruger, *J. Mol. Struct. THEOCHEM* **2002**, *577*, 281.
[30] V. Gokul, et al., *J. Mol. Struct. THEOCHEM* **2004**, *672*, 119.
[31] J. M. Fox, et al., *J. Org. Chem.* **2004**, *69*, 7317.
[32] H. G. Kruger, et al., *J. Mol. Struct. THEOCHEM* **2006**, *771*, 165.
[33] H. G. Kruger, P. S. Mdluli, *J. Struct. Chem.* **2006**, *17*, 121.
[34] M. M. Lawal, et al., *J. Mol. Model.* **2016**, *22*, 1.
[35] S. Yamabe, T. Ishikawa, *J. Org. Chem.* **1997**, *62*, 7049.
[36] D. M. Birney, P. E. Wagenseller, *J. Am. Chem. Soc.* **1994**, *116*, 6262.
[37] D. M. Birney, S. Ham, G. R. Unruh, *J. Am. Chem. Soc.* **1997**, *119*, 4509.
[38] D. M. Birney, X. Xu, S. Ham, *Angew. Chem. Int. Ed.* **1999**, *38*, 189.
[39] J. R. Pliego, J. M. Riveros, *J. Phys. Chem. A* **2001**, *105*, 7241.
[40] R. F. Ribeiro, et al., *J. Phys. Chem. B* **2011**, *115*, 14556.
[41] A. V. Marenich, C. J. Cramer, D. G. Truhlar, *J. Phys. Chem. B* **2009**, *113*, 6378.
[42] M. J. Frisch, et al., *Gaussian 09*, Gaussian, Inc., Wallingford, CT **2009**.
[43] A. D. Becke, *J. Chem. Phys.* **1993**, *98*, 1372.
[44] C. Lee, W. Yang, R. G. Parr, *Phys. Rev. B* **1988**, *37*, 785.

[45] X. Xu, W. A. Goddard, *Proc. Natl. Acad. Sci. U. S. A.* **2004**, *101*, 2673.
[46] J. P. Perdew, Y. Wang, *Phys. Rev. B* **1992**, *45*, 13244.
[47] Y. Zhao, N. González-García, D. G. Truhlar, *J. Phys. Chem. A* **2005**, *109*, 2012.
[48] Y. Zhao, D. G. Truhlar, *Acc. Chem. Res.* **2008**, *41*, 157.
[49] W. J. Hehre, R. Ditchfield, J. A. Pople, *J. Chem. Phys.* **1972**, *56*, 2257.
[50] M. J. Frisch, J. A. Pople, J. S. Binkley, *J. Chem. Phys.* **1984**, *80*, 3265.
[51] F. Weigend, R. Ahlrichs, *Phys. Chem. Chem. Phys.* **2005**, *7*, 3297.
[52] F. Weigend, *Phys. Chem. Chem. Phys.* **2006**, *8*, 1057.
[53] T. H. Dunning Jr, *J. Chem. Phys.* **1989**, *90*, 1007.
[54] D. E. Woon, T. H. Dunning Jr, *J. Chem. Phys.* **1995**, *103*, 4572.
[55] P. J. Hay, W. R. Wadt, *J. Chem. Phys.* **1985**, *82*, 270.
[56] W. R. Wadt, P. J. Hay, *J. Chem. Phys.* **1985**, *82*, 284.
[57] P. J. Hay, W. R. Wadt, *J. Chem. Phys.* **1985**, *82*, 299.
[58] R. E. Easton, et al., *Theor. Chim. Acta* **1996**, *93*, 281.
[59] J. Li, C. J. Cramer, D. G. Truhlar, *Theor. Chem. Acc.* **1998**, *99*, 192.
[60] C. Sosa, et al., *J. Phys. Chem.* **1992**, *96*, 6630.
[61] N. Godbout, et al., *Can. J. Chem.* **1992**, *70*, 560.
[62] J. W. Ochterski, *Vibrational Analysis in Gaussian*, help@gaussian.com, **1999**.
[63] C. Gonzalez, H. B. Schlegel, *J. Phys. Chem.* **1990**, *94*, 5523.
[64] R. Dennington, T. Keith, J. Millam, *GaussView*, Semichem Inc., Shawnee Mission, KS **2009**.
[65] J. D. Bradley, G. C. Gerrans, *J. Chem. Educ.* **1973**, *50*, 463.
[66] C.-G. Zhan, J. A. Nichols, D. A. Dixon, *J. Phys. Chem. A* **2003**, *107*, 4184.
[67] W. T. Yang, R. G. Parr, *Proc. Natl. Acad. Sci. U. S. A.* **1985**, *82*, 6723.
[68] M. Berkowitz, *J. Am. Chem. Soc.* **1987**, *109*, 4823.
[69] S. B. Liu, *J. Chem. Sci.* **2005**, *117*, 477.
[70] P. Politzer, D. G. Truhlar, *Chemical Applications of Atomic and Molecular Electrostatic Potentials: Reactivity, Structure, Scattering, and Energetics of Organic, Inorganic, and Biological Systems*, Springer Science & Business Media, **2013**.
[71] J. B. Foresman, A. Frisch, *Exploring Chemistry with Electronic Structure Methods*, 2nd ed., Gaussian, Inc., Pittsburgh, PA **1996**.
[72] C. M. Breneman, K. B. Wiberg, *J. Comput. Chem.* **1990**, *11*, 361.
[73] H. E. Baumgarten, in *Mechanism and Theory in Organic Chemistry* (Eds: T. H. Lowry, K. S. Richardson), ACS Publications, **1989**.
[74] M. B. Smith, J. March, *March's Advanced Organic Chemistry: Reactions, Mechanisms, and Structure*, John Wiley & Sons, **2007**.
[75] I. Alecu, et al., *J. Chem. Theory Comput.* **2010**, *6*, 2872.
[76] C. Bunton, J. Fendler, *J. Org. Chem.* **1966**, *31*, 2307.
[77] Z. Fakhar, et al., *J. Mol. Struct.* **2017**, *1128*, 94.
[78] L. P. Wolters, F. M. Bickelhaupt, *ChemistryOpen* **2012**, *1*, 96.
[79] C. P. Okoli, Q. J. Guo, G. O. Adewuyi, *Carbohydr. Polym.* **2014**, *101*, 40.
[80] P. Deglmann, A. Schafer, C. Lennartz, *Int. J. Quant. Chem.* **2015**, *115*, 107.
[81] R. McWeeny, *Proc. R. Soc. Lond. A: Math. Phys. Eng. Sci.*, The Royal Society, **1956**.
[82] P. K. Weiner, et al., *Proc. Natl. Acad. Sci.* **1982**, *79*, 3754.
[83] J. B. Hendrickson, D. J. Cram, G. S. Hammond, *Organic Chemistry*, McGraw-Hill, New York, NY **1970**.

SUPPORTING INFORMATION

Additional Supporting Information may be found online in the supporting information tab for this article.

How to cite this article: Lawal MM, Govender T, Maguire GEM, Kruger HG, Honarparvar B. DFT study of the acid-catalyzed esterification reaction mechanism of methanol with carboxylic acid and its halide derivatives. *Int J Quantum Chem.* 2018;118:e25497. https://doi.org/10.1002/qua.25497